Permeability of Phenol Through Cellulose Acetate Membranes by Reverse Osmosis in Various Alcoholic Systems

HIROSHI NOMURA, MANABU SENŌ, HIROSHI TAKAHASHI, and
TAKEO YAMABE, *Institute of Industrial Science, University of Tokyo,
Minato-ku, Tokyo 106, Japan*

Synopsis

Reverse osmosis separation of phenol in various alcoholic solutions using porous cellulose acetate membranes was investigated. The permeation behavior of phenol was measured for cellulose acetate membranes having various pore size distributions which were prepared by annealing at four different temperatures. Some differences were found between the aqueous and the alcoholic solutions in solute permeabilities and product rates. Membranes annealed at 90°C showed higher permselectivity than membranes annealed at lower temperatures. The pore character was classified into two types according to the relation of the product rate of 1-propanol and that of water. It was found in a series of alcoholic solutions that the permeability of phenol, the product rate, and the apparent partition coefficient are closely related to the carbon number of the alcohols, but the values of $J_v \times \eta$ (ca. 1.25 $\times 10^{-4}$ poise·m^3/m^2·day) and of the permselectivity coefficient (ca. 0.83) remain constant. The result was analyzed by using the three-dimensional solubility parameter to obtain some information for the partition mechanism of solutes in aqueous and alcoholic solutions.

INTRODUCTION

The purpose of this investigation is to elucidate the separation mechanism of organic solutes such as phenol and to discuss the factors that govern the solute permeabilities in the reverse osmosis process.

Lonsdale et al.[1] reported the enrichment of phenol in an aqueous solution by reverse osmosis, and Matsuura et al.[2] investigated the permeation behavior of phenol and found a correlation between the shift in OH-stretching vibration $\Delta\nu$ (or Taft's number $\Sigma\sigma^*$) and the permeation rate in the reverse osmosis process.

In this study, by using membranes annealed at different temperatures, the influence of the pore size distribution on permeabilities was examined. Moreover, the variation of solute permeabilities for various alcohol solutions was also discussed. Measurements were carried out for the permselectivity coefficients T_B^S by reverse osmosis and the solute partition coefficient Kd' by the column method described in a previous paper.[3]

In order to analyze the factors governing the behavior of solutes through the cellulose acetate membranes in the reverse osmosis process, the three-dimensional solubility parameter was used. The general background and applicability of the three-dimensional solubility parameter are described in the literature.[4-7] This parameter is developed on the assumption that the total cohesive energy E can be divided into three contributions from the dispersion forces E_d, the permanent dipole–permanent dipole forces E_p, and the hydrogen-bonding forces E_h. Thus,

0021-8995/79/0024-1191$01.00

$$E = E_d + E_p + E_h \tag{1}$$

By dividing this equation by the molar volume V, we obtain

$$\delta = \delta_d{}^2 + \delta_p{}^2 + \delta_h{}^2 \tag{2}$$

where $\delta = (E/V)^{1/2}$ is the three-dimensional solubility parameter, which is composed of three parts, δ_d, δ_p, and δ_h. The quantity E/V is called the internal pressure, or the cohesive energy density. If the values of the solubility parameters of two components are nearer to each other, they are more miscible with each other. The three-dimensional solubility parameter provides some information for the interaction between the membrane matrix and permeates.

EXPERIMENTAL

The apparatus used is the same as that described in the previous paper.[3] The circulating velocity of the feed solution was 24 l./hr, and the operating pressure was 100 kg/cm^2. Under these conditions, the effect of the concentration polarization near the membrane surface could be neglected, for the circulating velocity is much larger than the total product rate. The membranes used are porous cellulose acetate membranes of the Loeb–Sourirajan type, which were prepared by casting at room temperature from solutions of the following composition (wt.%): acetone, 45.0; cellulose acetate (degree of acetylation, 39.8%; Eastman Chemical Products, Inc., E-398-3), 25.0; formamide, 30.0.

For elucidation of the effects of the pore distribution on membrane performance, the following experiment was carried out. The membranes were treated by annealing at four different temperatures (60, 70, 80, and 90°C) in hot water for 5 min. The membrane properties were characterized by the measurements of salt rejection and product rate under conditions which are usually adopted for the aqueous system: feed solution, 5000 ppm aq. NaCl; and operating pressure, 40 kg/cm^2. For organic systems the product rate at a pressure of 40 kg/cm^2 is very small, and then the measurements were therefore operated at 100 kg/cm^2. The fractional solute permeability is independent of the operating pressure as described in the previous paper.[3] In order to discuss the membrane performances for the organic system, the solute permeability, the permselectivity coefficient, and the product rate were measured in a 0.05 mole/l. phenol–0.05 mole/l. benzene system where 1-propanol was used as a solvent.

The salt rejection Rej. (%) is determined by the relationship

Rej. (%)

$$= \frac{\text{salt concentration in feed} - \text{salt concentration in product}}{\text{salt concentration in feed}} \times 100 \tag{3}$$

The fractional solute permeability P_S is defined by the following equation:

$$P_S = \frac{\text{solute concentration in product}}{\text{solute concentration in feed}} \tag{4}$$

In the present investigation, benzene was selected as a reference solute, and the permselectivity coefficient T_B^S is defined as

$$T_B^S = \frac{\text{fractional solute permeability of a given solute S}}{\text{fractional solute permeability of benzene (reference)}} = \frac{P_S}{P_B} \tag{5}$$

For the reverse osmosis experiment, only a membrane named "CA-4" was used, the properties of which were discussed in the previous paper.[3] The concentration of the feed solution was 0.05 mole/l. phenol–0.05 mole/l. benzene, and some alcohols shown in Table I were used as solvent. The permselectivity coefficients T_B^S and the solute permeabilities were determined according to eqs. (4) and (5).

The solute partition coefficients Kd' were determined using a liquid chromatographic technique with the column packed with cellulose acetate powder from which the membranes were prepared. The method was described in detail in the previous paper.[3] The apparent solute partition coefficient Kd'^S is defined as

$$Kd'^S = \frac{\text{concentration of solute in unit volume of column}}{\text{concentration of solute in unit volume of mobile phase}} \quad (6)$$

In order to examine the changes in the apparent solute partition coefficient with the kind of alcohol, a series of primary alcohols as shown in Table I were used as eluents. The value of Kd' for 1-butanol solution could not measured because a steady flow through the column packed with the cellulose acetate particles could not obtained; this would be caused by a large pressure drop owing to the high viscosity of 1-butanal (ca. 2.5 cp).

RESULTS AND DISCUSSION

Effect of Pore Distribution on Membrane Performances for Organic System

The effect of pore distribution on the membrane performances was investigated by using cellulose acetate membranes annealed at different temperatures. The cellulose acetate membranes annealed at the higher temperatures have a pore distribution containing smaller pore sizes.

The salt rejections and the product rates of five kinds of cellulose acetate membranes unannealed and annealed at 60–90°C are shown in Figures 1 and 2. The feed solution is 5000 ppm NaCl aqueous solution, and the operating pressure is 40 kg/cm². The membrane annealed at 90°C shows very high salt rejection, but the product rate (0.04 m³/m²·day) decreases by about a tenth of that of the membrane annealed at 80°C. The general trend in the membrane performance is similar to that reported already in the literature.[8]

TABLE I
Characteristics of Alcohols

	Dipole moment[a] μ, debye	OH-Stretching[b] vibration shift $\Delta\nu$, cm^{-1}	Viscosity[c] η_{25}, cp	Density[c] d_{20}, g/cm³
Methanol	1.68 (22°C)	149	0.546	0.79
Ethanol	1.70 (24.5°C)	143	1.08	0.79
1-Propanol	1.69 (22°C)	141	1.98	0.80
1-Butanol	1.66 (22°C)	145	2.48	0.80

[a] In benzene, from ref. 10.

[b] In benzene, from ref. 2, obtained from the measurements of OH band maximum in carbon tetrachloride and ether solutions.
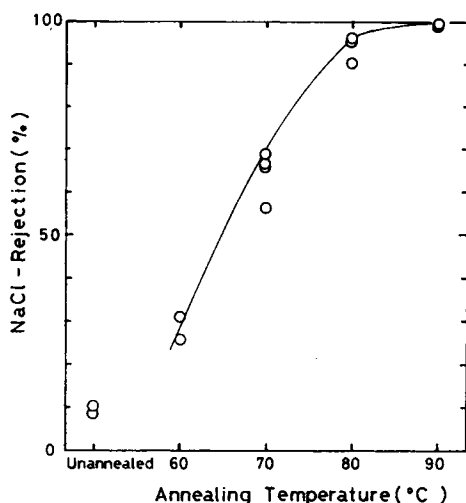
[c] In benzene, from ref. 11.

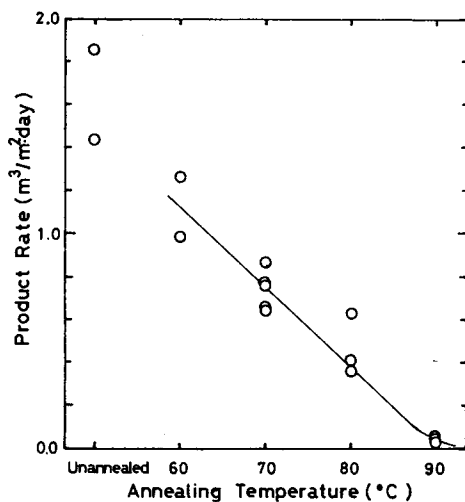Fig. 1. Effect of annealing temperature on NaCl rejection.

Fig. 2. Effect of annealing temperature on product rate.

With these membranes the effects of the pore size distribution on membrane performances for the organic system were investigated. The relationship between NaCl rejection and solute permeabilities in 1-propanol is shown in Figure 3. Up to a NaCl rejection of 95%, the permeabilities of phenol and benzene and the permselectivity coefficient (ca. $P_S = 1.01$, $P_B = 1.09$, and $T_B^S = 0.92$) do not change remarkably, but in the region of a salt rejection higher than 95%, the permeability of benzene increase and that of phenol decrease (ca. $P_S = 0.89$, $P_B = 1.13$, and $T_B^S = 0.79$). The result shows that the pore size distribution of the membranes annealed at 60 to 80°C do not remarkably affect the permselectivity of the organic solutes, but membranes annealed at 90°C have a pore distribution that exhibits a higher permselectivity for phenol.
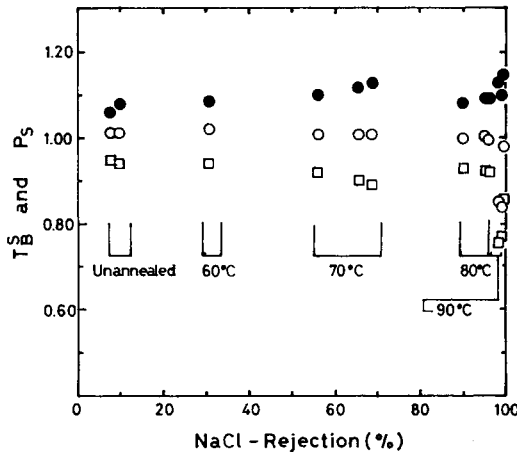
Fig. 3. Permselectivity coefficient T_B^S and permeability P_S vs NaCl rejection: (O) P_S(●) P_B; (□) T_B^S.

Relation Between Product Rates of 1-Propanol and Water

The pore character of the membrane was discussed by comparing the product rate in the aqueous system with that in the organic system.[9] The relationship observed in the present system is shown in Figure 4. Two kinds of pore character are classified, as indicated by the two dashed lines 1 and 2 in Figure 4. One is characterized typically by the unannealed membranes as designated by line 1, and the other is characterized by the membrane annealed at 80 and 90°C, as designated by line 2. Membranes annealed at 60 and 70°C lie between lines 1 and 2. By annealing the membrane at higher temperatures, the pore character changes from class 1 to class 2, and the membrane performance is improved considerably.

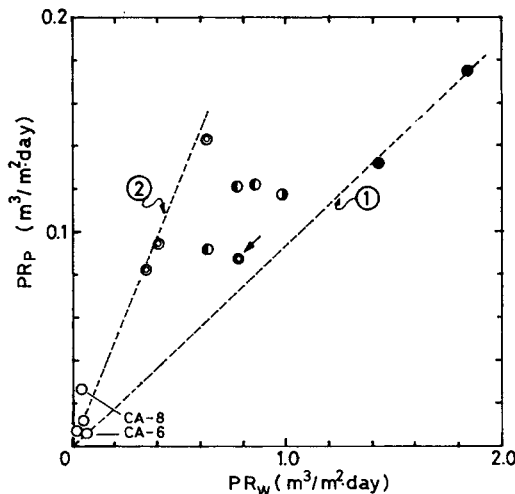Sometimes, it was observed that membranes annealed at the higher temper-

Fig. 4. Determination of pore character by comparing product rate of 1-propanol, PR_p, with that of water, PR_W: (●) unannealed; (◐) 60°C; (◑) 70°C; (◎) 80°C; (O) 90°C. ① class 1, characterized by unannealed membranes; ② class 2, characterized by membranes annealed at 80 and 90°C.

atures did not show good performances such as lower salt rejection and larger product rate. For example, the 80°C-annealed membrane, indicated by the arrow in Figure 4, shows a NaCl rejection of 51.2% and a product rate of 0.75 $m^3/m^2 \cdot day$. This is probably due to the difference in pore character as discussed later.

By comparing the product rate of water with that of 1-propanol, the membranes can be classified into two classes. Most of the membranes annealed at 90°C lie on line 2 and belong to class 2. But there are exceptional membranes such as "CA-6" which lie on line 1. A comparison of the membrane performances of CA-6 and CA-8 is shown in Table II. The order of the product rates of water and 1-propanol is inverse. This would be due to the difference in pore character. The pores in the active layer created by annealing have high salt-rejecting performance. These pore surfaces have a high density of active groups. On the other hand, the pores formed originally during membrane preparation have surfaces that are poorer in activity, although they are somewhat shrunken by annealing. The poor salt rejection of CA-6 and the 80°C-annealed membrane marked by the arrow would result from such a pore character.

There is no remarkable difference in the permeability of benzene between class 1 and class 2. This means that the solute permeability in the organic system is primarily determined by the pore size of the membrane and is not affected by the pore character, while the solvent flux is largely influenced by the pore character of the membrane.

Relation Between Product Rate and Carbon Number of Alcohols

The change in the product rate with the carbon number of alcohols is shown in Figure 5. The product rate decreases steeply with increase in carbon number of the alcohols. The following equation holds for the product rate:

$$J_v = A \ \Delta P \tag{7}$$

where J_v is the product rate, ΔP is the operating pressure difference, and A is a coefficient. The values of A depend on the viscosity η of the alcohols used as solvent. Thus, if

$$A = A'/\eta \tag{8}$$

then

$$J_v = (A'/\eta)\Delta P \tag{9}$$

If the values of A' and ΔP are constant, the following relationship would hold:

TABLE II
Performances of Two Types of Cellulose Acetate Membranes at 25°C

Membrane	Product rate of water,[a] $(m^3/m^2 \cdot day) \times 10^{-2}$	Salt rejection,[a] %	Product rate of 1-propanol,[b] $(m^3/m^2 \cdot day) \times 10^{-2}$	Permeability of benzene[b]
CA-6	6.09	79.9	0.70	1.14
CA-8	4.19	99.5	2.69	1.15

[a] Feed, 5000 ppm NaCl aqueous solution; operating pressure, 40 kg/cm^2.

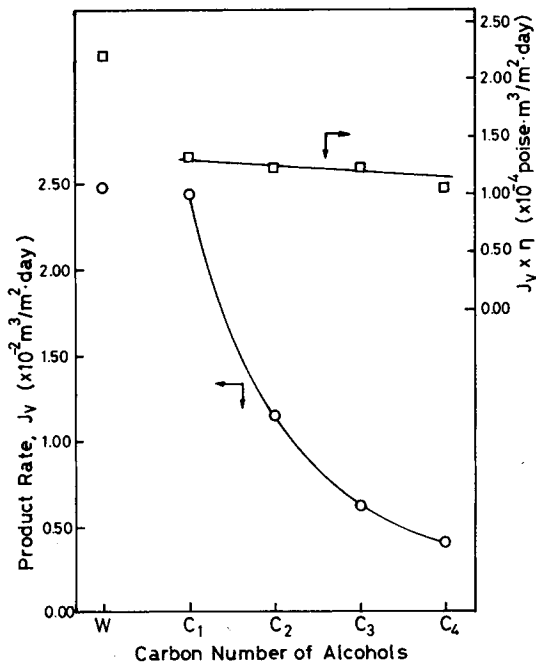[b] Feed, 0.05 mole/l. benzene in 1-propanol; operating pressure, 100 kg/cm^2.

Fig. 5. Relationship between product rate and carbon number of alcohols: Membrane, CA-4; W, water; C_1, methanol; C_2, ethanol; C_3, 1-propanol; C_4, 1-butanol; operating pressure, 100 kg/cm^2.

$$J_v \times \eta = \text{const.} \tag{10}$$

As shown in Figure 5, the product of J_v and η is nearly constant, about 1.25×10^{-4} poise·m^3/m^2·day for C_1 to C_4 alcohols. The result supports the above relationship.

The value of $J_v \times \eta$ of water (2.20×10^{-4} poise·m/day) is very different from those of alcohols. The difference from the alcoholic systems is due to the difference in the character of permeate flow, as described in the last section.

Solute Permeabilities and Permselectivities

The variation of the behavior of solute permeation with the carbon number of alcohols is shown in Figure 6 and 7. As shown in Figure 6, the solute fluxes of benzene and phenol decrease with increasing carbon number of alcohols, and the solute flux of phenol in the aqueous system lies on the line extrapolated from the alcoholic systems. On the other hand, as shown in Figure 7, the value of the fractional solute permeability of benzene is 1.00 for the ethanol solution, and at this point the permeation behavior changes from rejection to enrichment. For the permeation of phenol, the point $P_s = 1$ is realized for 1-butanol solution. In spite of the variation in fractional solute permeabilities, the permselectivity coefficients of phenol against benzene remain constant for four alcoholic solutions.

A negative rejection of phenol is observed for aqueous solution; the fractional solute permeability P_S of phenol shows a value of 1.33, which is very different from the trend of variation in values for alcoholic solutions. This is due to the difference in the flow character between phenol and water. As shown in Figure
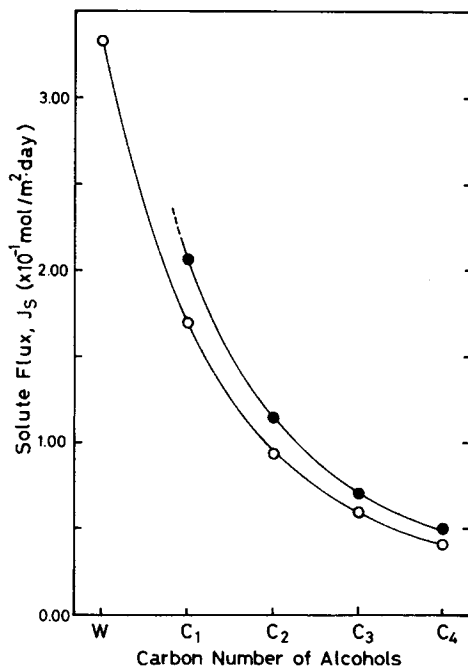
Fig. 6. Relationship between solute flux, J_S, and carbon number of alcohols; membrane, CA-4; W, water; C_1, methanol; C_2, ethanol; C_3, 1-propanol; C_4, 1-butanol; (O) phenol; (●) benzene; operating pressure, 100 kg/cm^2.

6, the flow of phenol as solute has the same trend as that of alcohols, while the flow of water as solvent deviates from that of the alcohol systems as shown in Figure 5, and therefore the permeability of phenol in water does not have the value expected from the alcohol series.

Relation Between Solute Permeability and Apparent Solute Partition Coefficient

The variations in the apparent solute partition coefficient Kd'^S and the logarithm of the ratio of the apparent solute partition coefficient, log (Kd'^S/Kd'^B), with the carbon number of the alcohols are shown in Figure 8. The solute partition coefficients increase with increase in the carbon number of the alcohols. In spite of the variation in the solute partition coefficients, the ratio of the apparent solute partition coefficient of phenol to that of benzene is constant. This correlation is similar to that between the solute permeabilities and the permselectivity coefficients as shown in Figure 7. This result suggests that the partition coefficient Kd is a dominant factor determining the permeation behavior of the organic solute, as described in the previous paper.[3]

Analysis of Solute Partition Behavior in Terms of Solubility Parameter

The solubility parameters of related compounds and cellulose acetate are listed in Table III. In this study, the three-dimensional solubility parameters were used. The diagram of solubility parameter on the δ_h–δ_p plane is shown in Figure
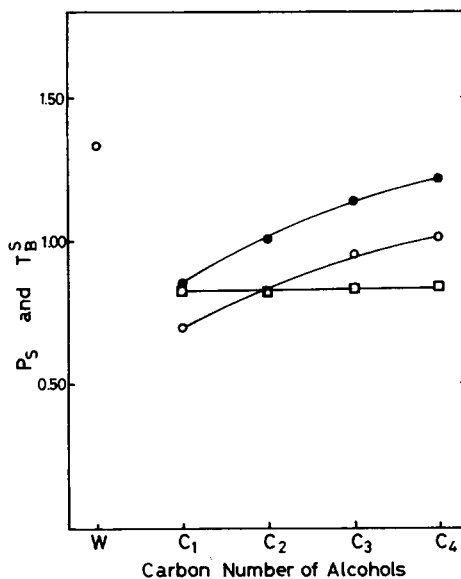
Fig. 7. Variation in solute permeability P_S and permselectivity coefficient T_B^S with carbon number of alcohols: membrane, CA-4; W, water; C_1, methanol; C_2, ethanol; C_3, 1-propanol; C_4, 1-butanol. T_B^S: ($\square$), P_S: (O) phenol; ($\bullet$) benzene; operating pressure, 100 kg/cm^2.
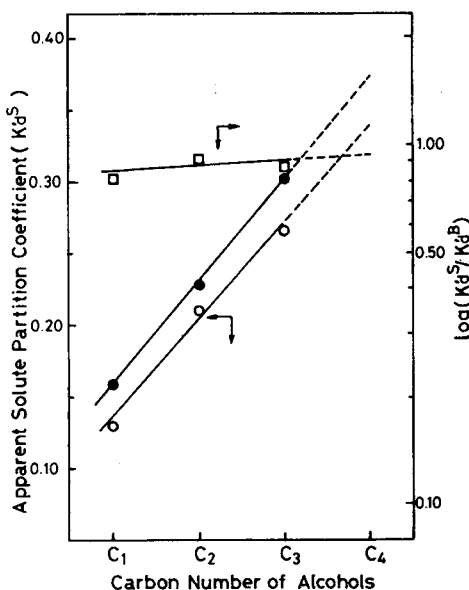

Fig. 8. Variation in apparent solute partition coefficient Kd'^S with carbon number of alcohols: column, CA(E-398-3). Eluent: C_1, methanol; C_2, ethanol; C_3, 1-propanol; C_4, 1-butanol. Kd'^S: (O) phenol; ($\bullet$) benzene.

9. For analysis of organic substances, the term from the dispersion force, δ_d, is nearly constant and could be ignored in almost all cases. Then, the two terms of the solubility parameter, δ_h and δ_p, are discussed on the δ_h–δ_p plane. The distance between two spacies on the δ_h–δ_p plane serves as a measure for the degree of affinity between them. The shorter the distance between two organic
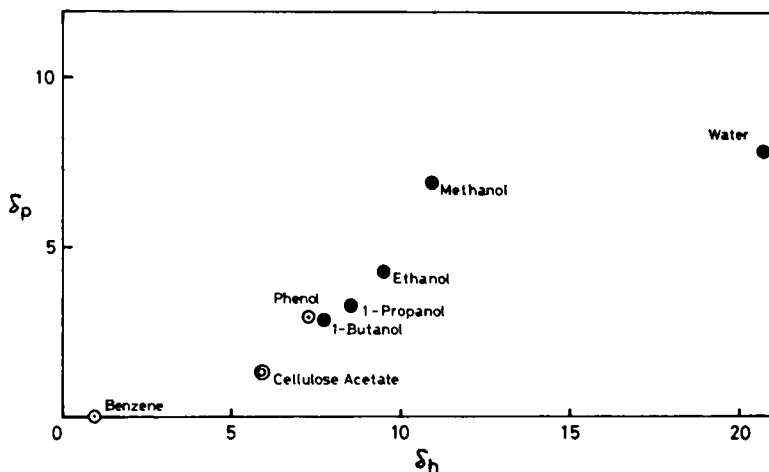
Fig. 9. Solubility parameter diagram on δ_h–δ_p plane.

species, the greater the affinity between them. The distance D is given by the following equation:

$$D = (\Delta\delta_p{}^2 + \Delta\delta_h{}^2)^{1/2} \qquad (12)$$

where

$$\Delta\delta_p = \delta_{p1} - \delta_{p2} \qquad \Delta\delta_h = \delta_{h1} - \delta_{h2} \qquad (13)$$

The results of the partition behavior shown in Figure 8 do not agree simply with the prediction from the affinity measured by the solubility parameter. Therefore, the model of partition equilibrium behavior as shown in Figure 10 should be proposed. For the analysis of the partition equilibrium of solute in dilute solutions, the ratio of amount of solute/solvent together with the affinity between the solute and the polymer matrix should be taken into consideration. For the partition equilibrium of phenol in alcohol systems, the ratio of the amount is more important, for the difference in the affinities between phenol and alcohol to the cellulose acetate particles is not large. On the other hand, the affinity term is more important for aqueous systems, for the affinity of phenol to the cellulose

TABLE III
Solubility Parameters of Related Compounds and Cellulose Acetate

	Molar volume	Solubility parameter			
		δ	δ_d	δ_p	δ_h
Water	18.0	23.4	7.6	7.8	20.7
Methanol	40.7	14.6	7.7	6.0	10.9
Ethanol	58.5	13.0	7.8	4.3	9.5
1-Propanol	75.2	12.0	7.8	3.3	8.5
1-Butanol	91.5	11.3	7.8	2.8	7.7
Benzene	89.4	9.1	9.0	0	1.0
Phenol	87.5	11.8	8.8	2.9	7.3
Cellulose acetate[b]	—	10.5	8.6	1.3	5.9

[a] From ref. 6.
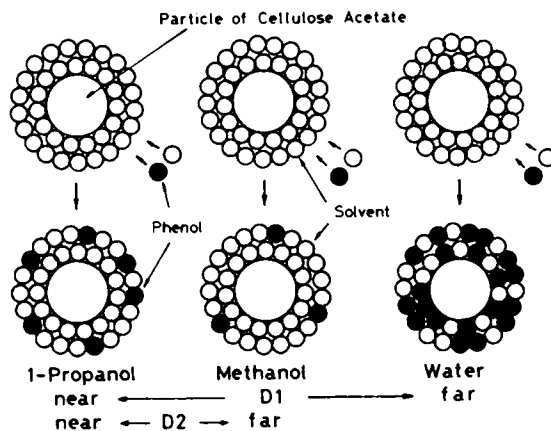[b] Calculated by the method of ref. 5.

Fig. 10. Model for partition behavior of solvent and solute molecules on cellulose acetate particles. Dl is the solubility parameter distance between solvent and cellulose acetate and D2 is the solubility parameter distance between solvent and phenol. The large spheres represent cellulose acetate particles, and the solute and solvent molecules which surround the particles are represented as small spheres, of which open circles are molecules of solvent (alcohol or water) and filled circles are molecules of solute (phenol). In alcoholic solvents the particles are exclusively surrounded by alcohol, whereas in aqueous systems the water molecules surrounding the particle are partly replaced by phenol molecules.

acetate particles is much greater than that of water. These considerations are illustrated in Figure 10. The solvent molecules which surround the cellulose acetate particles are partially replaced by the solute molecules to attain partition equilibrium. In alcoholic systems, the partition of phenol onto the particles is relatively low, because the affinity of alcohol for cellulose acetate is comparable to that of phenol and the amount of alcohol is more abundant. As a result, the nature of the cellulose acetate particles is primarily governed by the property of the alcohol. Figure 11 shows the relationship between the apparent solute
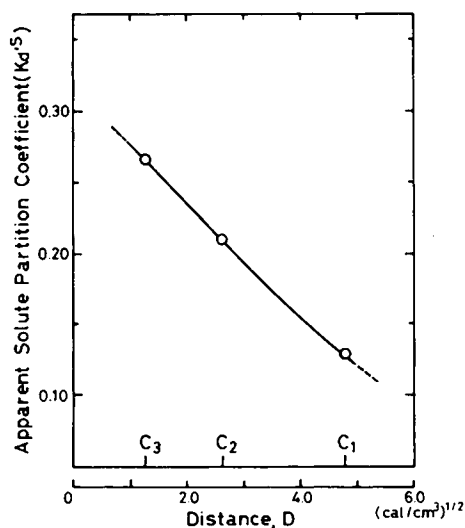

Fig. 11. Relationship between apparent solute partition coefficient of phenol, Kd'^S, and distance D on $\delta_h-\delta_p$ plane: C_1, methanol; C_2, ethanol; C_3, 1-propanol.

partition coefficient and the distance D, which is measured as the distance between phenol and alcohol adsorbed on the cellulose acetate particles. The result agrees with the above consideration.

A similar relation holds for the partition of benzene between the solvent layer on the particles and the solution phase, as shown in Figure 12.

For the aqueous system, the partition of phenol onto the particles is high because of the low affinity of water for cellulose acetate. The situation is illustrated in Figure 10. This is the reason why phenol is concentrated in aqueous systems while it is rejected in alcoholic systems.

CONCLUSIONS

It is clear from the results described in the preceding sections that there are some differences in the permeation mechanism between the aqueous system and the alcoholic system. The influential factors are the pore character of the membrane and the partition behavior of the solute. For characterization of the pore structure of the membrane, the relationship of the product rate of 1-propanol and that of water is available. On the other hand, an analysis in terms of the three-dimensional solubility parameter is useful for explanation of the partition behavior.

For a series of alcoholic solutions, the solute permeabilities, the product rate, and the apparent partition coefficient are closely related to the carbon number of alcohols used as solvents, but the values of $J_v \times \eta$ and the permselectivity coefficient are constant. These relations are useful for the prediction of the permeation behavior of other series of organic substances.

Furthermore, the results of the apparent partition coefficient obtained by the liquid chromatography column method serve as useful prediction for the reverse osmosis separation of organic compounds in various media.
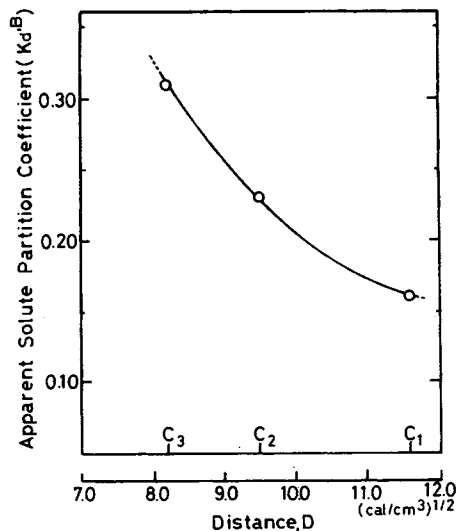

Fig. 12. Relationship between apparent solute partition coefficient of benzene, Kd'^S, and distance D on δ_h–δ_p plane: C_1, methanol; C_2, ethanol; C_3, 1-propanol.

References

1. H. K. Lonsdale, U. Merten, and M. Tagami, *J. Appl. Polym. Sci.*, **11,** 1807 (1967).

2. T. Matsuura and S. Sourirajan, *J. Appl. Polym. Sci.*, **16,** 1663 (1972).

3. H. Nomura, S. Yoshida, M. Senō, H. Takahashi, and T. Yamabe, *J. Appl. Polym. Sci.*, **22,** 2609 (1978).

4. C. M. Hansen, *Ind. Eng. Chem., Res. Develop.*, **8,** 2 (1969).

5. D. M. Koenhem and C. A. Smolders, *J. Appl. Polym. Sci.*, **19,** 1163 (1975).

6. C. M. Hansen and A. Beerbower, *Encyclopedia of Chemical Technology, Supplement*, Interscience, New York, 1971, p. 889.

7. A. S. Chawla and T. M. S. Chang, *J. Appl. Polym. Sci.*, **19,** 1723 (1975).

8. S. Sourirajan, *Reverse Osmosis,* Logos Press, London, 1971.

9. H. Ohya, H. Konuma, and Y. Negishi, *J. Appl. Polym. Sci.*, **21,** 2515 (1977).

10. Landolt-Børnstein, *Physikalisch-Chemische Tabellen*, 6th ed., Vol. I/3, Springer-Verlag, Berlin, 1951, p. 386.

11. Landolt-Børnstein, *Physikalisch-Chemische Tabellen*, 5th ed., Vol. I, Springer-Verlag, Berlin, 1923, pp. 126 and 366.

12. R. E. Rathbun and A. L. Babb, *J. Phys. Chem.*, **65,** 1072 (1961).

13. D. W. McCall and D. C. Douglass, *J. Chem. Phys.*, **32,** 1876 (1960).